

A high-order conservative remap for DG schemes on curvilinear polygonal meshes

Konstantin Lipnikov Nathaniel Morgan

Los Alamos National Laboratory

April 29, 2019, Marseille, FRANCE

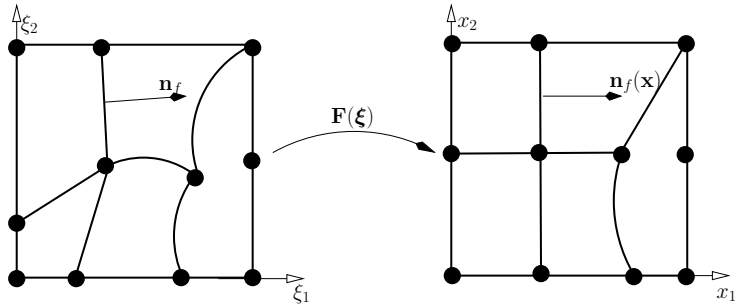


- ① Problem formulation**
- ② Summary of main results**
- ③ Virtual element space and projectors**
- ④ Numerical examples**
- ⑤ Summary**

- ① Write equations in a moving frame
- ② Advance physical fields in time
- ③ Improve mesh quality
- ④ Transfer fields to the improved mesh
- ⑤ Goto to step 2.

Problem formulation (1/3)

We are looking for algorithms that transfer **conservatively** DG fields from a Lagrangian (left) to a relaxed (right) mesh:



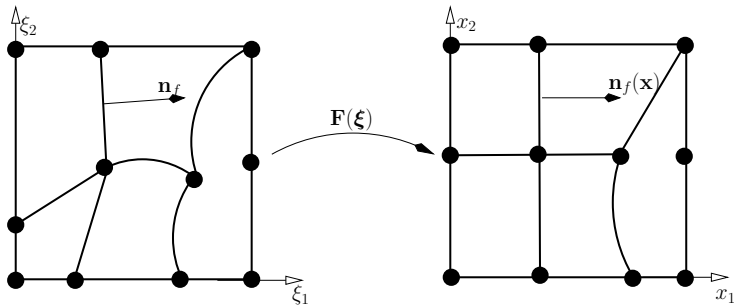
Space-time map:

$$\mathbf{x}(\xi, \tau) = \xi + \tau(\mathbf{F}(\xi) - \xi)$$

Remap velocity:

$$\mathbf{u} = \frac{\partial \mathbf{x}}{\partial \tau}$$

Problem formulation (2/3)



$$\mathbf{u} = \frac{\partial \mathbf{x}}{\partial \tau}, \quad \mathbf{x}(\xi, \tau) = \xi + \tau(\mathbf{F}(\xi) - \xi)$$

Assumptions:

- ① **\mathbf{u} is known only on the mesh edges.**
- ② **\mathbf{u} is a polynomial.**

Problem formulation (3/3)

Consider a scalar field ρ (e.g. density):

$$0 = \frac{\partial \rho}{\partial \tau} = \frac{d\rho}{d\tau} - \mathbf{u} \cdot \nabla \rho$$

Thus, the PDE formulation of the remap problem is

$$\frac{d\rho}{d\tau} = \mathbf{u} \cdot \nabla \rho$$

Taylor basis

$$\rho_h|_c = \rho_0^c + \rho_1^c \psi_1^c + \rho_2^c \psi_2^c + \rho_3^c \psi_3^c + \dots$$

where

$$\psi_0^c(\boldsymbol{\xi}) = 1$$

$$\psi_1^c(\boldsymbol{\xi}) = a_1^c(\xi_1 - \xi_{1,c})$$

$$\psi_2^c(\boldsymbol{\xi}) = a_2^c(\xi_2 - \xi_{2,c})$$

$$\psi_i^c(\boldsymbol{\xi}) = a_i^c [(\xi_1 - \xi_{1,c})^{\alpha_1} (\xi_2 - \xi_{2,c})^{\alpha_2} - b_i^c \psi_0^c]$$

The coefficients a_i^c and b_i^c are defined from

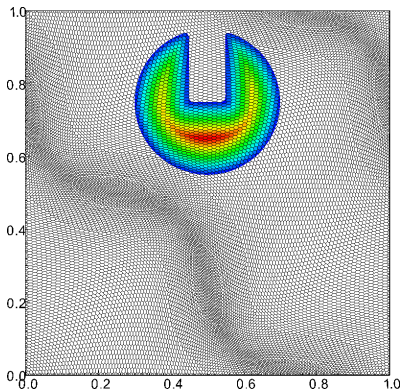
$$\int_c \psi_0^c \psi_i^c d\xi = |c| \delta_{0,i} \quad \text{and} \quad \int_c |\psi_i^c|^2 d\xi = |c|$$



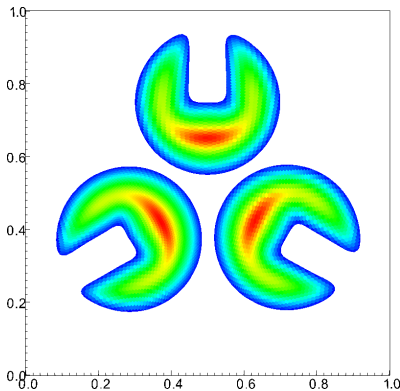
What should we expect? (1/2)

DG shows excellent performance for a similar linear advection equation:

$$\frac{\partial \phi}{\partial t} + \mathbf{u} \cdot \nabla \phi = 0, \quad \mathbf{u} = (y, -x)^T.$$



$t = 0$

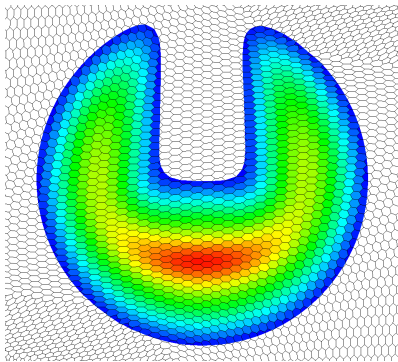


$t = 2.1, 4.2, 2\pi$

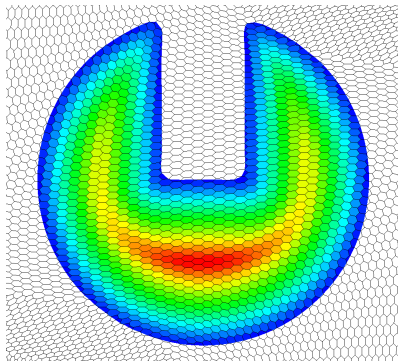


What should we expect (2/2)

High-order DG reduces significantly numerical diffusion which is critical for solutions with sharp features:



$\mathbf{DG}(\mathcal{P}^1)$



$\mathbf{DG}(\mathcal{P}^2)$

Main results for the remap problem

$$\frac{d\rho}{d\tau} = \mathbf{u} \cdot \nabla \rho$$

- ① Locally conservative modal DG schemes
- ② High-order DG schemes, $k = 1, 2, 3$
- ③ Treatment of curvilinear meshes
- ④ Conservative BJ-type limiter

Weak formulation (1/3)

For a (discontinuous) test function ψ , we have

$$\begin{aligned}\frac{d}{d\tau} \sum_c \int_{c(\tau)} \rho \psi \, dx = & - \sum_c \int_{c(\tau)} (\mathbf{u} \cdot \nabla \psi) \rho \, dx \\ & + \sum_f \int_{f(\tau)} (\mathbf{u} \cdot \mathbf{n}) \rho^*[\psi] \, dx\end{aligned}$$

Here '*' is a downwind approximation and we assumed that the basis function is constant on characteristics, i.e.

$$\frac{d\psi}{d\tau} = 0$$



Weak formulation (2/3)

Change to the reference frame introduces the Jacobian matrix \mathbb{J} and its determinant j :

$$\begin{aligned} \frac{d}{d\tau} \sum_c \int_{c(0)} \rho \psi j \, d\xi = \\ - \sum_c \int_{c(0)} (\mathbf{u} \cdot j \mathbb{J}^{-t} \nabla_\xi \psi) \rho \, d\xi \\ + \sum_f \int_{f(0)} (\mathbf{u} \cdot j \mathbb{J}^{-t} \mathbf{n}) \rho^*[\psi] \, d\xi \end{aligned}$$

Weak formulation (3/3)

Approximation of unknown objects j , \mathbb{J} , and \mathbf{u} :

$$\begin{aligned} \frac{d}{d\tau} \sum_c \int_{c(0)} \rho \psi \mathcal{I}_{c,1}(j) d\xi = \\ - \sum_c \int_{c(0)} (\mathcal{I}_{\text{c}}(\mathbf{u}) \cdot \mathcal{I}_{c,2}(j \mathbb{J}^{-t}) \nabla_\xi \psi) \rho d\xi \\ + \sum_f \int_{f(0)} (\mathbf{u} \cdot j \mathbb{J}^{-t} \mathbf{n}) \rho^*[\psi] d\xi \end{aligned}$$

Simplification: $\mathcal{I}_{c,i}$ are derived from \mathcal{I}_c :

$$\mathbb{J} \rightarrow \mathbb{J}_h = \mathbf{I} + \tau \nabla_\xi (\mathcal{I}_{\text{c}}(\mathbf{u})), \quad j \rightarrow j_h = \det(\mathbb{J}_h)$$



Find $\rho_h \in \mathbf{DG}(\mathcal{P}^k)$ **s.t. for any** $\psi_h \in \mathbf{DG}(\mathcal{P}^k)$ **we have**

$$\begin{aligned}\frac{d}{d\tau} \sum_c \int_{c(0)} \rho_h \psi_h j_h \, d\xi = \\ - \sum_c \int_{c(0)} (\mathcal{I}_c(\mathbf{u}) \cdot j_h \mathbb{J}_h^{-1} \nabla_\xi \psi_h) \rho_h \, d\xi \\ + \sum_f \int_{f(0)} (\mathbf{u} \cdot j \mathbb{J}^{-1} \mathbf{n}_f) [\psi_h] \rho_h^* \, d\xi.\end{aligned}$$

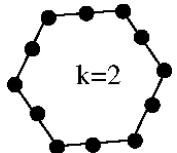
We use a TVD RK3 scheme for time stepping.

Let $\mathbf{u} \cdot \mathbf{n} = 0$ on the boundary. Taking $\psi_h = 1$, we obtain:

$$\frac{d}{d\tau} \sum_c \int_{c(0)} \rho_h j_h \, d\xi = 0.$$

Consider the serendipity virtual element space of order k :

$$\begin{aligned} \mathcal{V}_k(c) = \left\{ \mathbf{v} \in C^0(\bar{c}) : \quad & \mathbf{v}|_f \in \mathcal{P}^k(f) \quad \forall f \in \partial c, \\ & \Delta \mathbf{v} \in \mathcal{P}^k(c), \right. \\ & \int_c \mathbf{v} \cdot \mathbf{q} \, d\xi = \int_c \mathcal{L}\mathcal{S}_c(\mathbf{v}) \cdot \mathbf{q} \, d\xi \quad \forall \mathbf{q} \in \mathcal{P}^k(c) \left. \right\} \end{aligned}$$



- The least-square operator $\mathcal{L}\mathcal{S}_c(\mathbf{v})$ is the L^2 projector for this space.
- The virtual space is globally continuous.

Elliptic projector in the virtual space

We define the projector $\mathcal{I}_c(\mathbf{u}) \in \mathcal{P}^k(c)$ by

$$\int_c (\nabla_\xi \mathcal{I}_c(\mathbf{u}) - \nabla_\xi \mathbf{u}) \cdot \nabla_\xi \mathbf{q} \, d\xi, \quad \forall \mathbf{q} \in \mathcal{P}^k(c)$$

subject to

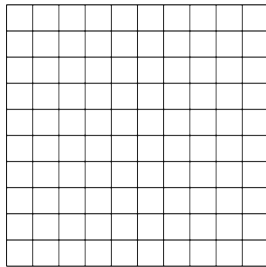
$$\int_c \mathcal{I}_c(\mathbf{u}) \, d\xi = \int_c \mathbf{u} \, d\xi.$$

- $\mathcal{I}_c(\mathbf{u})$ is the H^1 projector for this space
- It is **computable**, see VE/mimetic literature
- Quasi-optimality is due to

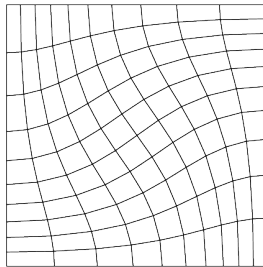
$$\|\nabla_\xi \mathcal{I}_c(\mathbf{u})\|_{L^2(c)} \leq \|\nabla_\xi \mathbf{u}\|_{L^2(c)}$$



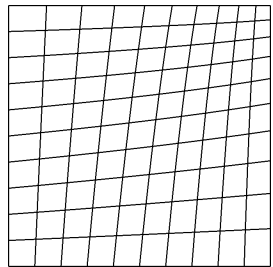
Example of meshes: logically square



Original



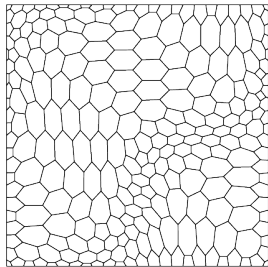
TG map



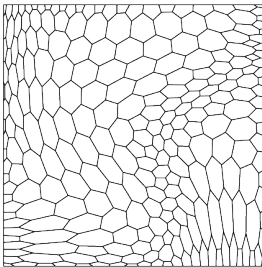
CE map

TG = Taylor-Green vorticial motion
CE = Compression/Expansion

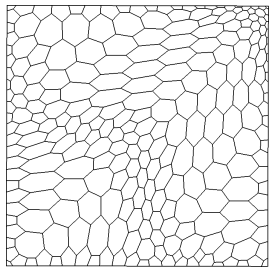
Example of meshes: polygonal



Original



TG map

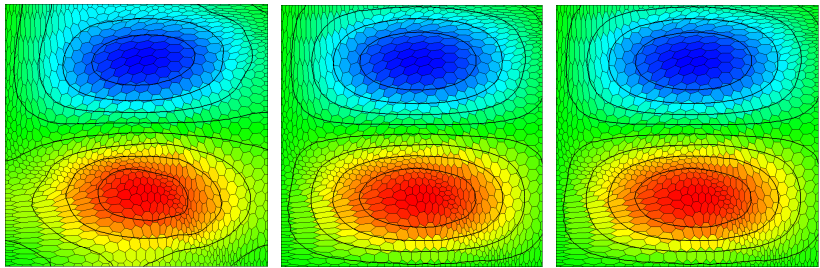


CE map

TG = Taylor-Green vorticial motion
CE = Compression/Expansion

Analytic solution

$$\rho(\xi_1, \xi_2) = \sin(6\xi_1) \sin(3\xi_2)$$



The TG map on polygonal meshes in $DG(\mathcal{P}^k)$ schemes with $k = 0, 1, 2$

Convergence (1/2)

$$\rho(\xi_1, \xi_2) = \sin(6\xi_1) \sin(3\xi_2)$$

	DG(\mathcal{P}^0)		DG(\mathcal{P}^1)		DG(\mathcal{P}^2)	
	L^2	L^∞	L^2	L^∞	L^2	L^∞
16^2	1.43e-1	4.31e-1	1.98e-2	7.85e-2	1.57e-3	9.31e-3
32^2	8.13e-2	3.57e-1	4.69e-3	1.94e-2	1.79e-4	1.15e-3
64^2	4.67e-2	2.73e-1	1.14e-3	4.66e-3	2.13e-5	1.38e-4
128^2	2.68e-2	1.99e-1	2.81e-4	1.17e-3	2.61e-6	1.84e-5
rate	0.805	0.372	2.046	2.028	3.077	3.001

TG map on polygonal meshes



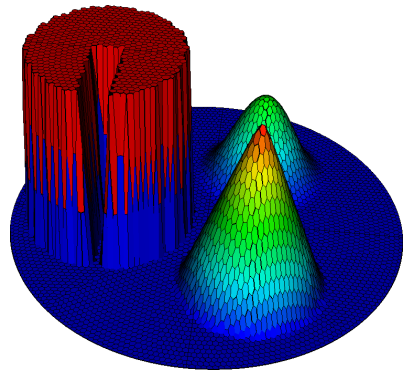
Convergence (2/2)

$$\rho(\xi_1, \xi_2) = \sin(6\xi_1) \sin(3\xi_2)$$

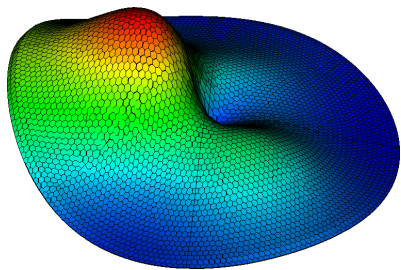
	DG(\mathcal{P}^0)		DG(\mathcal{P}^1)		DG(\mathcal{P}^2)	
	L^2	L^∞	L^2	L^∞	L^2	L^∞
16^2	1.23e-1	4.15e-1	2.03e-2	8.58e-2	1.67e-3	1.40e-2
32^2	6.43e-2	2.25e-1	4.92e-3	2.87e-2	1.94e-4	1.82e-3
64^2	3.35e-2	1.64e-1	1.21e-3	7.24e-3	2.41e-5	2.21e-4
128^2	1.75e-2	1.23e-1	3.01e-4	1.81e-3	3.06e-6	2.77e-5
rate	0.937	0.571	2.025	1.867	3.027	2.998

CE map on polygonal meshes. Factor 200 in CPU performance in favor of DG(\mathcal{P}^1) Factor 14 in favor of DG(\mathcal{P}^2)

Poor performance of the lowest-order scheme



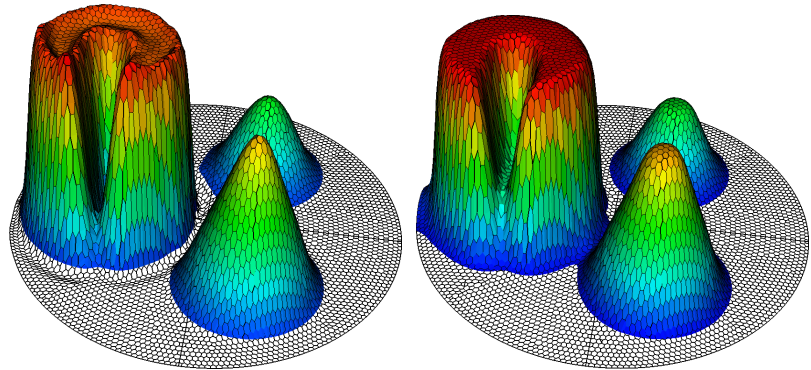
Initial solution



Unlimited DG(\mathcal{P}^0)

The lowest-order solution is diffused significantly after 360° rotation of the mesh

Impact of limiters (1/2)

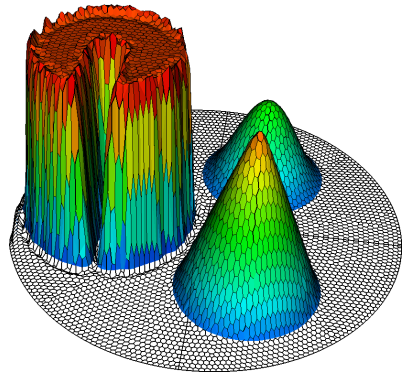


Unlimited $DG(\mathcal{P}^1)$

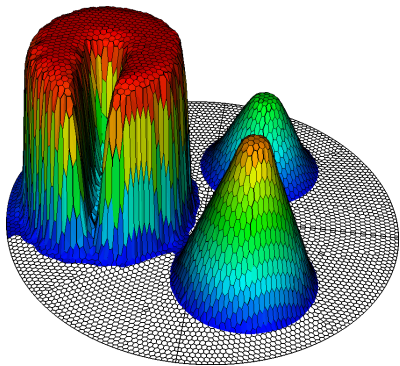
Limited $DG(\mathcal{P}^1)$

**3 shapes (cylinder, cone, hump) on the mesh
of polygons after 360° rotation of the mesh**

Impact of limiters (2/2)



Unlimited $DG(\mathcal{P}^2)$



Limited $DG(\mathcal{P}^2)$

**3 shapes (cylinder, cone, hump) on the mesh
of polygons after 360° rotation of the mesh**

① Select a scaling coefficients:

$$\hat{\rho}_h|_c = \rho_0^c + \alpha_c (\rho_1^c \psi_1^c + \rho_2^c \psi_2^c + \rho_3^c \psi_3^c + \dots)$$

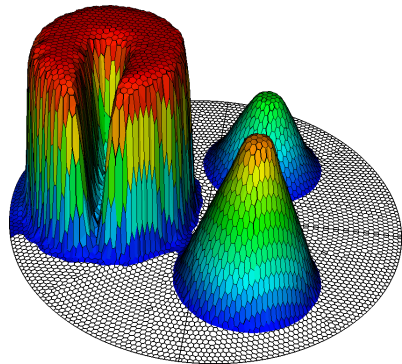
where $0 \leq \alpha_c \leq 1$ is such that

$$\min_{c' \in \mathcal{F}_c} \{\rho_0^{c'}\} \leq \hat{\rho}_h(\xi_k) \leq \max_{c' \in \mathcal{F}_c} \{\rho_0^{c'}\}, \quad \forall \xi_k \in \mathcal{G}_c^{k_1}$$

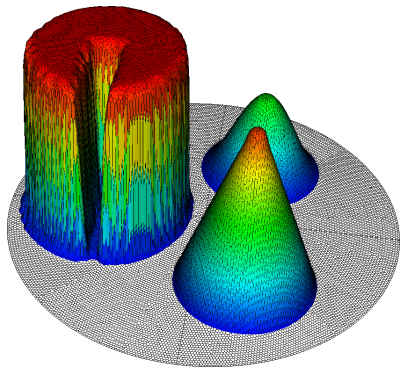
② Restore the local conservation:

$$\hat{\rho}_0^c = \alpha_c \rho_0^c + (1 - \alpha_c) \frac{1}{|c(\tau)|} \int_{c(0)} \rho_h j_h \, dV.$$

Impact of resolution



Limited DG(\mathcal{P}^2)



Limited DG(\mathcal{P}^2)

Impact of mesh resolution: better plateau and kinks; same roundness of the cylinder brims.



- Developed high-order DG schemes for the remap problem using the virtual element method.
- The schemes handle curvilinear polygonal meshes.
- Developed a conservative Barth-Jespersen-type limiting strategy for discontinuous functions.
- Future work: extend the scheme to 3D.
- Future work: shock capturing algorithms.